J. Fluid Mech. (1995), *vol.* 282, *pp.* 233–245

Stability of eccentric core–annular flow

By ADAM HUANG AND DANIEL D. JOSEPH

Aerospace Engineering and Mechanics, University of Minnesota, 110 Union St. S.E., Minneapolis, MN 55455, USA

(Received 24 January 1994 and in revised form 4 August 1994)

Perfect core–annular flows are two-phase flows, for example of oil and water, with the oil in a perfectly round core of constant radius and the water outside. Eccentric core flows can be perfect, but the centre of the core is displaced off the centre of the pipe. The flow is driven by a constant pressure gradient, and is unidirectional. This kind of flow configuration is a steady solution of the governing fluid dynamics equations in the cases when gravity is absent or the densities of the two fluids are matched. The position of the core is indeterminate so that there is a family of these eccentric core flow steady solutions. We study the linear stability of this family of flows using the finite element method to solve a group of PDEs. The large asymmetric eigenvalue problem generated by the finite element method is solved by an iterative Arnoldi's method. We find that there is no linear selection mechanism; eccentric flow is stable when concentric flow is stable. The interface shape of the most unstable mode changes from varicose to sinuous as the eccentricity increases from zero.

1. Introduction

Motivated by the possibility of lubricating one fluid by another, two-phase pipeflow has been widely studied. Although two-phase flows are very complicated and the interface separating the phases is very irregular in general, there is a tendency for two fluids to arrange themselves so that the less-viscous phase is in the region of high shear. In a pipeflow the less-viscous fluid goes to the wall and the high-viscosity phase stays in the centre. Thus by introducing a small amount of lubricant one can greatly reduce the drag, as in the case of lubrication of heavy crudes by water.

Experiments to explore this possibility have been carried out by Russell & Charles (1959), Charles, Goviers & Hodgson (1961) and Oliemens & Ooms (1986) among many others. A comprehensive review of results can be found in the monograph by Joseph & Renardy (1992). A more recent experimental study by Arney *et al.* (1993) identifies correlations for the friction factor and holdup ratios which fit all available data. Among all the realized flow patterns, core–annular flow has the greatest volume flux for a given pressure drop. The pressure drop along the pipe can be even smaller than the pressure drop in water alone at the same value of the volume flux.

Various flow types such as oil bubbles and slugs in water, wavy core flows, perfect core flows, etc. can be studied by stability theory. While early flow models were usually overidealized, more and more realistic models have been studied recently with the help of high-speed computers (see Joseph & Renardy 1992). Examples of such works are Joseph, Renardy & Renardy (1983), Preziosi, Chen & Joseph (1989) and Hu & Joseph (1989). Their results are fairly inclusive for the case of perfect core–annular flow, in which the viscous core is perfectly concentric, with its centre coinciding with that of the pipe. Perfect core–annular flow is usually unstable owing to the following three kinds of instability: (*a*) capillary instability, (*b*) instability caused by interfacial friction and

(*c*) instability due to Reynolds stress. A small window of parameters was found in which perfect core–annular flow can be stable.

In horizontal flows, when the densities of water and oil are different, the core must be off-centre. What usually happens in experiments is a flow configuration where the core is wavy and slightly off-centre, 'flying' in the water without touching the wall. The mechanism of the navigation of the core and the relation between the position of the core centre and the density difference are not yet well understood. We know that secondary flow must be present to counteract the buoyancy and a wavy interface is essential. Perfect eccentric core flows are exact solutions of the governing equations when the oil and water have the same density so that gravity cannot act. These flows form a family of steady solutions with the position of the core as a control parameter. Huang, Christodoulou & Joseph (1994) have calculated friction factor *vs.* Reynolds number and holdup curves for perfect eccentric core flows in both laminar and turbulent cases. Eccentricity leads to only moderate increases of the friction. Since an eccentric core flow can be regarded as a disturbance to the perfect core–annular flow, we pose the question: in the case when the perfect core–annular flow is stable, is the slightly eccentric flow unstable?

A convenient way to frame this problem is to identify the domain of parameters in which concentric core flow is stable and study the stability of the neighbouring eccentric flows. This kind of study is routine in principle but difficult to carry out in practice; to do it we extended the Arnoldi numerical algorithm to the complex domain. The result of our numerical study is of considerable interest since it shows that the non-uniqueness of a perfect core with regard to the centre of the core in the density matched case is not removed by stability to small disturbances. If concentric core flow is stable, so are all the neighbouring eccentric core flows. This implies that all previous analysis of linear stability of concentric core flows were only a part of the story because eccentric core flows are equally good candidates for linear stability analysis. Since the qualitative picture of the stability of concentric core flows is not changed by eccentricity when the flow is stable, we may hope for qualitative similarity even when concentric flow is unstable. Our numerical results do suggest a certain similarity between unstable concentric and eccentric flows.

Turning next to a description of the numerical method we use to study stability, we note that the eccentric position of the core breaks the axisymmetry of the perfect core–annular flow. This lack of symmetry greatly increases the difficulty of the study of stability. Firstly, there is no closed form solution for the basic flow. Secondly, the usual decomposition in polar coordinates (r, θ, z) is no longer valid. A bipolar decomposition with normal z-modes can be imagined but is probably not practical. Therefore a group of PDEs has to be solved for the eigenvalue problem. Consequently, in order to solve these PDEs any numerical method, such as the finite element method we use here, will usually generate large asymmetric matrices (say, greater than 2000×2000). Conventional eigenroutines to calculate the eigenvalues with the largest imaginary parts of these big matrices are not available, and the calculation of all the eigenvalues is very inefficient. Special methods have to be introduced.

A common way to avoid directly solving all the eigenvalues of large matrices is by projection. Since the early 1950s, several projection methods have been developed to handle the eigenvalue problem of large sparse non-symmetric matrices. These are usually iterative methods based upon Krylov subspace techniques. Depending on the different deflation and preconditioning procedures used, there are many variations of the basic methods. For a good reference, see Saad (1989). The method we used here was originally developed by Saad (1980, 1989). It is an iterative Arnoldi algorithm

combined with a Schur–Wielandt deflation technique. Its application to hydrodynamic stability analysis has been successful (see Christodoulou & Scriven 1988). Saad's code was originally written for real matrices. For our case we slightly modified the code to handle the complex matrices generated from the finite element method. The resulting code is quite general for applications in hydrodynamic stability analysis, especially when the flow region is infinite in one or two dimensions. Before discussing numerical methods, we introduce the basic eccentric steady flow in a pipe.

2. The steady flow solutions

Consider a straight circular pipe filled with two immiscible fluids. The flow is driven by a constant pressure gradient along the axis of the pipe. The two fluids have different viscosities and interfacial tension acts on the interface. To exclude the effect of gravity, we assume that they have the same density.

The equations of motion are

$$\rho \frac{\mathrm{d}\hat{U}}{\mathrm{d}t} = -\nabla \hat{p} + \mu_l \Delta \hat{U}, \quad \nabla \cdot \hat{U} = 0, \tag{1}$$

where $l = 1, 2$ refers to the two fluids. We also require that

$$\hat{U} = 0 \text{ on the pipe wall.} \tag{2}$$

The equations on the interface $r = R(x, y, z, t)$ are

$$\hat{u} = \frac{\partial R}{\partial t} + \hat{U} \cdot \nabla R, \tag{3}$$

$$[\![\hat{U}]\!] = 0, \tag{4}$$

and

$$-([\![\hat{P}]\!] + 2HT)\,\boldsymbol{n} + [\![2\mu \boldsymbol{D}(\hat{U})]\!] \cdot \boldsymbol{n} = 0, \tag{5}$$

where $\boldsymbol{D}(\hat{U}) = \frac{1}{2}(\nabla \hat{U} + \nabla \hat{U}^T)$ and $[\![\cdot]\!] = (\cdot)_1 - (\cdot)_2$ is the jump across the interface, $2H$ is the mean curvature of the interface and $\boldsymbol{n}$ is the normal point from the core to the annulus.

We look for steady solutions of this system in which one phase of the fluid forms a core (fluid 1) with the lubricating fluid (2) outside. Neither the stratified case nor the case when there are several cores are considered here. We seek a two-phase Poiseuille flow with the only non-zero velocity component $W(x, y)$ independent of z. The governing equations for this solution are

$$\mu_l \nabla^2 W = f, \tag{6}$$

$$W = 0 \text{ on the wall,} \tag{7}$$

and the velocity and the shear stress are continuous across the interface:

$$[\![W]\!] = 0, \tag{8}$$

$$[\![\mu\, \partial W / \partial n]\!] = 0. \tag{9}$$

The normal stress balance on the interface is

$$[\![P]\!] + 2H\sigma = 0, \tag{10}$$

where σ is the interfacial tension coefficient. The pressure jump $[\![P]\!]$ is a constant. This implies that H is a constant and hence the interface separating the two phases is a cylinder. However, the position and the radius R_1 of the core have to be prescribed to specify the geometry of the flow domain. The position of the core can be simply described by the eccentricity of its centre, which is denoted as e, as shown in figure 1.

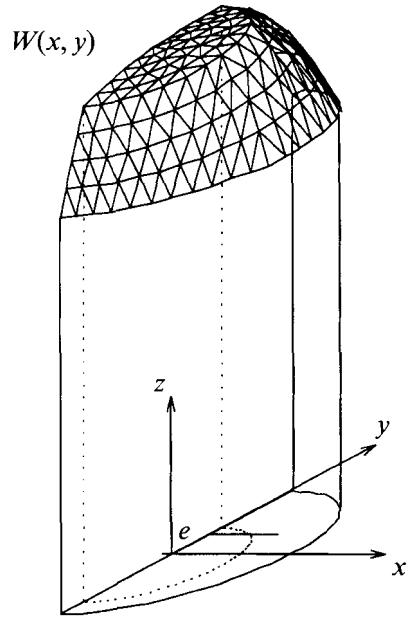

FIGURE 1. The basic solution for the case when $m = 0.05$, $e = 0.2$, $a = 0.6$.

Equation (6) is a Poisson equation with interface jump conditions. Bentwich (1964) solved this problem using bipolar coordinates and the solution was expressed as a type of Fourier series. It is convenient for our stability analysis to solve (6) with a simple finite element code. The nodal values of W will serve as the basic flow profile in the stability analysis. A sample of the mesh and the flow profile are shown in figure 1.

3. Equations for small disturbances

We now introduce small disturbances (u, v, w, p, δ) of the basic steady solution $(0, 0, W, P, R_1)$. The linearized equations satisfied by (u, v, w, p, δ) are

$$\frac{\partial u}{\partial x}+\frac{\partial v}{\partial y}+\frac{\partial w}{\partial z}=0, \tag{11}$$

$$\rho\left(\frac{\partial u}{\partial t}+W\frac{\partial u}{\partial z}\right)=-\frac{\partial p}{\partial x}+\mu\nabla^2 u, \tag{12}$$

$$\rho\left(\frac{\partial v}{\partial t}+W\frac{\partial v}{\partial z}\right)=-\frac{\partial p}{\partial y}+\mu\nabla^2 v, \tag{13}$$

$$\rho\left(\frac{\partial w}{\partial t}+u\frac{\partial W}{\partial x}+v\frac{\partial W}{\partial y}+W\frac{\partial w}{\partial z}\right)=-\frac{\partial p}{\partial z}+\mu\nabla^2 w. \tag{14}$$

δ is the disturbance of the radius R_1 and is a function of x, y, z and t. Let $\boldsymbol{n}$ be the outward normal of this disturbed interface:

$$\boldsymbol{n}=\frac{\nabla R(x,y,z,t)}{|\nabla R(x,y,z,t)|}. \tag{15}$$

$\boldsymbol{n}$ can be linearized as

$$\boldsymbol{n}=n_x\boldsymbol{i}+n_y\boldsymbol{j}+\boldsymbol{k}+O(\delta), \tag{16}$$

where n_x and n_y are the zeroth-order components of $\boldsymbol{n}$ in the x- and y-directions,

respectively, and they are independent of δ. We also introduce a unit tangent vector τ of the interface, pointing counterclockwise in the (x, y)-plane of the cross-section. Then we can write out the interface jump conditions satisfied by (u, v, w, p, δ) as follows:

$$\frac{\partial \delta}{\partial t} - n_x u - n_y v + W \frac{\partial \delta}{\partial z} = 0, \tag{17}$$

$$[\![u]\!] = 0, \tag{18}$$

$$[\![v]\!] = 0, \tag{19}$$

$$[\![w]\!] + \left[\!\!\left[\frac{\partial W}{\partial n}\right]\!\!\right] \delta = 0, \tag{20}$$

$$\left[\!\!\left[\mu\left(n_x\left(\frac{\partial v}{\partial n} + \frac{\partial u}{\partial \tau}\right) - n_y\left(\frac{\partial u}{\partial n} - \frac{\partial v}{\partial \tau}\right)\right)\right]\!\!\right] - [\![\mu]\!] \frac{\partial W}{\partial \tau} \frac{\partial \delta}{\partial z} = 0, \tag{21}$$

$$\left[\!\!\left[\mu\left(\frac{\partial w}{\partial n} + n_x \frac{\partial u}{\partial z} + n_y \frac{\partial v}{\partial z}\right)\right]\!\!\right] + \left[\!\!\left[\mu \frac{\partial^2 W}{\partial^w n}\right]\!\!\right] \delta - \frac{\partial \delta}{\partial \tau}\left[\!\!\left[\mu \frac{\partial W}{\partial \tau}\right]\!\!\right] = 0, \tag{22}$$

$$\left[\!\!\left[-p + 2\mu\left(n_x \frac{\partial u}{\partial n} + n_y \frac{\partial v}{\partial n}\right)\right]\!\!\right] = \sigma\left(\frac{\partial^2 \delta}{\partial^2 \tau} + \frac{\partial^2 \delta}{\partial^2 z} + \frac{\delta}{R_1^2}\right). \tag{23}$$

To make the above equations dimensionless we scale lengths with the radius of the pipe R, velocity with

$$W_0 = f[R_1^2(\mu_2 - \mu_1) + R^2 \mu_1]/4\mu_1 \mu_2, \tag{24}$$

which is the centreline velocity in the concentric case. For comparison we use W_0 as our velocity scale even in the eccentric case. Time is scaled with R/W_0 and pressure with ρW_0^2. The following dimensionless parameters appear in the dimensionless equations:

$$\text{Reynolds number: } Re_l = \rho W_0 R/\mu_l,$$

$$\text{viscosity ratio: } m = \mu_2/\mu_1,$$

$$\text{dimensionless core radius: } a = R_1/R,$$

$$\text{interfacial tension number: } J^* = \rho\sigma R/\mu_1^2.$$

To keep the nomenclature short, we use the same symbols for the dimensionless and dimensional variables. Consider (u, v, w, p, δ) to be dimensionless now. After introducing the normal mode

$$\begin{bmatrix} u(x,y,z,t) \\ v(x,y,z,t) \\ w(x,y,z,t) \\ p(x,y,z,t) \\ \delta(x,y,z,t) \end{bmatrix} = \begin{bmatrix} u(x,y) \\ v(x,y) \\ iw(x,y) \\ p(x,y) \\ i\delta(x,y) \end{bmatrix} \exp[\mathrm{i}\alpha(z - ct)]$$

into the linearized equations, we find that

$$\frac{\partial u}{\partial x} + \frac{\partial v}{\partial y} - \alpha w = 0, \tag{25}$$

$$\mathrm{i}\alpha(W - c)\, u = -\frac{\partial p}{\partial x} + \frac{1}{Re_l}(\nabla^2 - \alpha^2)\, u, \tag{26}$$

$$\mathrm{i}\alpha(W - c)\, v = -\frac{\partial p}{\partial y} + \frac{1}{Re_l}(\nabla^2 - \alpha^2)\, v, \tag{27}$$

$$-\alpha(W - c)\, w + u \frac{\partial W}{\partial x} + v \frac{\partial W}{\partial y} = -\mathrm{i}\alpha p + \frac{\mathrm{i}}{Re_l}(\nabla^2 - \alpha^2)\, w, \tag{28}$$

where α is the wavenumber, c is the eigenvalue and the Laplacian is two-dimensional. The imaginary pat of c will determine the stability of the basic state. On the boundary, u, v, w are zero. The interface conditions are

$$\alpha(W-c)\,\delta + n_x u + n_y v = 0, \tag{29}$$

$$\left[\!\left[m\left(n_x\left(\frac{\partial v}{\partial n}+\frac{\partial u}{\partial \tau}\right)-n_y\left(\frac{\partial u}{\partial n}-\frac{\partial v}{\partial \tau}\right)\right)\right]\!\right] + \alpha(1-m)\frac{\partial W}{\partial \tau} = 0, \tag{30}$$

$$\left[\!\left[m\left(\frac{\partial w}{\partial n}+\alpha(n_x u+n_y v)\right)\right]\!\right] + \left[\!\left[m\frac{\partial^2 W}{\partial^2 n}\right]\!\right]\delta - \frac{\partial \delta}{\partial \tau}\left[\!\left[m\frac{\partial W}{\partial \tau}\right]\!\right] = 0, \tag{31}$$

$$\left[\!\left[-p+\frac{2}{Re}\left(n_x\frac{\partial u}{\partial n}+n_y\frac{\partial v}{\partial n}\right)\right]\!\right] = -\mathrm{i}J^*\left(\frac{\partial^2 \delta}{\partial^2 \tau}-\alpha^2\delta+\frac{\delta}{a^2}\right), \tag{32}$$

where $m_1 = 1, m_2 = m$. Equations (18), (19) and (20) remain the same.

We note that the partial derivatives with respect to τ in the interface equations and the derivatives of W in the field equations are associated with the eccentric position of the core and vanish in concentric flow. This makes it impossible to fully separate the variables and reduce the governing equations to ODEs. One could imagine that there might be some way to further simplify the equations by using bipolar coordinates but we prefer to solve this system of equations numerically, since there are many related stability problems which can only be solved numerically. This relatively simple problem might as well serve as a test ground for the numerical algorithms needed for the study of eigenvalue problems for PDEs.

4. Numerical methods

The system governing the disturbances (u, v, w, p, δ) is an eigenvalue problem. Using the same mesh as for the calculation of the basic flow, we discretize this system by the finite element approximation. Special attention is paid to the interfacial equations since they cannot always be incorporated into the main equations in the weak form of the system (see Hu & Joseph 1989). Also, equations such as (32) are ordinary differential equations for δ, which is only defined on the basic interface. We have to treat them as extra constraints with the normal derivatives of (u, v, w) on the interface as extra unknowns. This makes the mass matrices from the finite element approximation asymmetric, which in turn greatly increases the difficulty for the eigenvalue solver.

The resulting matrix equation is a generalized eigenvalue problem of the form

$$\boldsymbol{M}\boldsymbol{q} = c\boldsymbol{B}\boldsymbol{q}, \tag{33}$$

where $\boldsymbol{M}$ is non-singular. $\boldsymbol{B}$ is usually a singular matrix because some of the equations do not contain the time derivatives. The number of nodes needed to resolve the basic steady flow and the disturbances proves to be such that the dimension N of $\boldsymbol{M}$ and $\boldsymbol{B}$ is at least 2000 and possibly more, depending on the values of the parameters such as viscosity ratio, Reynolds number and so on. Thus the matrices are large, but they are banded because of the so-called near orthogonality of the basic shape functions. A great effort was made in labelling the nodes of the mesh in order to reduce the bandwidth of $\boldsymbol{M}$ and $\boldsymbol{B}$.

Because only the eigenvalues with the largest imaginary part determine the stability of the basic flow it would be very inefficient to apply the general library routines, which compute all the eigenvalues, to the above system. The common way of avoiding this inefficiency is to use subspace projection methods. As Saad (1989) pointed out, there

have been three basic approaches to the projection methods. The one we shall use is the so-called Arnoldi's method. The idea behind all the projection methods is to approximate an eigenvector $\boldsymbol{u}$ by a vector $\boldsymbol{x}$ of a subspace K by orthogonal Galerkin projection, so that the residual vector of $\boldsymbol{x}$ is orthogonal to another subspace, which may be the same K. More precisely, for an eigenvalue system

$$\boldsymbol{A}\boldsymbol{u} = \lambda \boldsymbol{u}, \tag{34}$$

where $\boldsymbol{A}$ is an $n \times n$ complex matrix, we look for an approximate eigenpair $(\mu, \boldsymbol{x})$ in $C \times K$. K is an k-dimensional subspace of C^n, provided that

$$\boldsymbol{v}^c \cdot (\boldsymbol{A} - \mu)\boldsymbol{x} = 0, \quad \forall \boldsymbol{v} \in K. \tag{35}$$

Arnoldi's method uses the Krylov subspace as K, which is defined as

$$K = \text{span}(\boldsymbol{v}_1, \boldsymbol{A}\boldsymbol{v}_1, \boldsymbol{A}^2\boldsymbol{v}_1, \ldots, \boldsymbol{A}^{(k-1)}\boldsymbol{v}_1), \tag{36}$$

where $\boldsymbol{v}_1$ belongs to C^n and has unitary Euclidean norm. Let $\boldsymbol{v}_1, \boldsymbol{v}_2, \ldots, \boldsymbol{v}_k$ be k orthogonal vectors of K, and $\boldsymbol{V}_k$ be the matrix composed with $\boldsymbol{v}_i$ as its columns. Then we can write

$$\boldsymbol{x} = \boldsymbol{V}_k \boldsymbol{y}, \quad \boldsymbol{y} \in C^k. \tag{37}$$

Thus (35) is equivalent to

$$\boldsymbol{V}_k^H (\boldsymbol{A} - \mu)\boldsymbol{x} = 0, \tag{38}$$

or

$$(\boldsymbol{V}_k^H \boldsymbol{A} \boldsymbol{V}_k - \mu)\boldsymbol{y} = 0. \tag{39}$$

Note that $\boldsymbol{V}_k^H \boldsymbol{A} \boldsymbol{V}_k$ in (39) is a $k \times k$ matrix, which is to be solved routinely. Its eigenvalues provide the approximations to the eigenvalues of $\boldsymbol{A}$ and the eigenvectors are related by (37).

The generalized problem (33) can be transformed to a system

$$(\boldsymbol{M} - \sigma \boldsymbol{B})^{-1} \boldsymbol{M} \boldsymbol{q} = \zeta \boldsymbol{q}, \tag{40}$$

whose eigenvalue ζ is related to λ by formula

$$\zeta = \frac{\lambda}{\lambda - \sigma}, \tag{41}$$

where σ, a complex number, is called a shift. Saad (1980, 1989) proved that $(\mu, \boldsymbol{x})$ is a good approximation to the original eigenpair for the outermost part of the spectrum of the system. From (41) this property is used in choosing the shift σ, i.e. the number closest to the desired eigenvalue is picked as the shift. Of course, the eigenvalue is not known beforehand; hence, in practice, a so-called shift- and invert strategy is adopted, which is essentially an iterative way to better approximate the eigenvalues. Adding this shift-and-invert process to the original algorithm will usually better separate the spectrum of the problem and accelerate the convergence.

5. Comparison with the concentric case

By combining Arnoldi's method with the shift-and-invert strategy and other transformation techniques, computer codes have been developed (Saad 1989). Their first application to the hydrodynamic stability problem was done by Christodoulou & Scriven (1988). We adapted Saad's code to complex matrices for use in our problem. We shall first compare the results with existing results.

Concentric core flow (also called perfect core–annular flow) is a special case of our general setup, in which the eccentricity is zero and axisymmetry allows the equations

$(Re_1, \alpha, m, J^*, a) =$	(10000, 1, 1, 0, 0.5)	(37.78, 10, 0.5, 0, 0.7)	(500, 5, 0.05, 1000, 0.9)
Salwen & Grosch	0.9717 − 0.02838i	—	—
Hu & Joseph	—	0.6693 + 0.004131i	0.3854 + 0.02087i
Arnoldi's method	0.9694 − 0.02867i (2401 × 2401)	0.6685 + 0.004332i (2087 × 2087)	0.4058 + 0.02511i (2002 × 2002)
	0.9699 − 0.02864i (2736 × 2736)	0.6689 + 0.004149i (2535 × 2535)	0.3837 + 0.02087i (2498 × 2498)

TABLE 1. Comparison of computer values of the most unstable eigenvalue for one-fluid Poiseuille flow and two-fluid core–annular flow with those obtained by Arnoldi's method

to be further reduced to ODEs by introducing the azimuthal modes proportion to $\exp(in\theta)$. The resulting equations were solved by different numerical schemes and the results have been summarized in Joseph & Renardy (1992). An even more special case is the one-fluid pipe flow problem, which can be obtained from the two-fluid model when the viscosity of the fluids is the same and the interfacial tension is zero. As is well-known, Poiseuille pipe flow is stable in the linear case, for which Salwen & Grosch (1972) have given some complete results for the leading eigenvalues. Table 1 is a comparison of the leading eigenvalues they computed for these special cases with those from our PDE code.

In table 1, the numbers in the brackets under each entry are the matrix size in our general program. The first row is for the case of pipe Poiseuille flow with results for Salwen & Grosch (1972); the second and third rows are for perfect core–annular flow; the results are taken from Hu & Joseph (1989). In our calculation for these test cases the dimension of Krylov subspace k is usually taken to be around 20, and in many instances only one pass of the iterative Arnoldi method is needed; for 2000×2000 matrices this takes about 10 s on the 8-CPU Cray YMP at the Minnesota Supercomputer Center. Since the shift strategy involves the inversion of the mass matrix, a fair amount of time spent on the LU decomposition in Arnoldi's method.

6. Results

Preziosi *et al.* (1989) and Hu & Joseph (1989) have shown that there are basically three types of instability of the perfect core–annular flow. One is the so-called capillary instability due to the interfacial tension, which stabilizes short-wave disturbances and destabilizes long-wave disturbances. This instability occurs at low Reynolds numbers. The second instability is associated with the viscosity difference between the two fluids and is due to interfacial friction. The third is the usual Reynolds stress instability for single-phase flow. The interfacial friction and the Reynolds stress instabilities occur at higher Reynolds number. Hence, there are two branches of the neutral curve: an upper and lower branch (see figure 8 of Preziosi *et al.* 1989). In general these two branches overlap so that there is no stability for most of the parameters. However, there is a small window of parameters in which the upper and lower branches of the neutral curve do not intersect and the perfect core–annular arrangement can be stable. We introduced some small eccentricity of the core for a case corresponding to figure 3 of Hu & Joseph (1989) and computed the neutral curves. Figure 2 shows the result when $J^* = 1000$, $m = 0.1$, and $a = 0.8$. The eccentricity is 0.02 and 0.05. It is clear that the neutral curves for slightly eccentric configurations are topologically identical to the ones for the concentric arrangement, although the upper branch becomes broader in

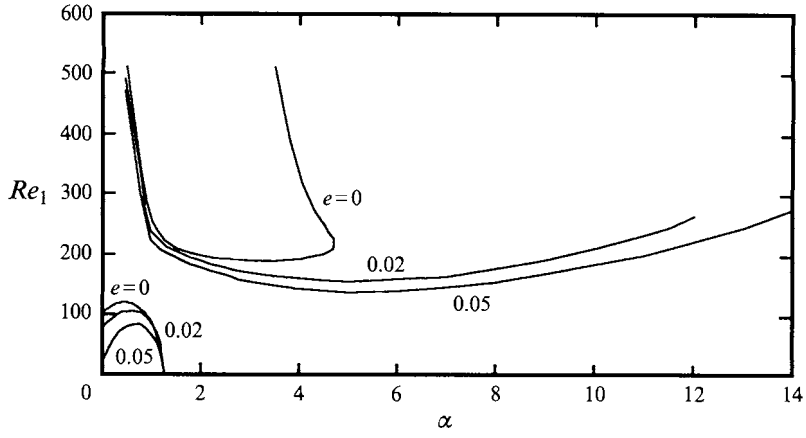

FIGURE 2. Neutral curves when $J^* = 1000$, $m = 0.1$, $a = 0.8$ and $e = 0$, 0.02, 0.05.

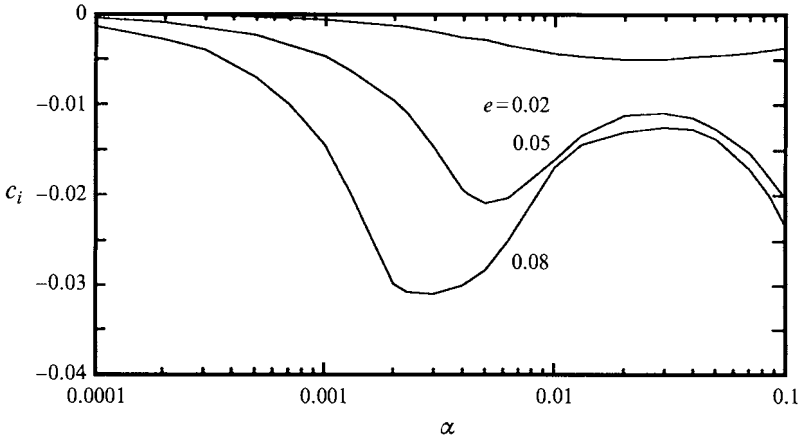

FIGURE 3. Long-wave modes for $J^* = 1000$, $m = 0.1$, $a = 0.8$ and $e = 0.02$, 0.05, 0.08, c_i is the maximum imaginary part of the eigenvalues.

the eccentric cases. Because of the nature of Arnoldi's method, one cannot obtain the whole spectrum of the problem at once. In our calculations, we always tried to scan the spectrum to make sure that no unstable eigenvalues were missed. No new modes of instability appear to arise for eccentric flow. Hence, eccentric flows can be stable in a window of parameters in which concentric flow is stable. Although the size of the stable window depends upon the eccentricity, under the right conditions a number of eccentric core flow configurations can be stable. Since each of these stable flows can be viewed as a disturbance of a neighbouring stable flow, they must all be neutrally stable. To make this clear, we recall that analysis of long-wave disturbances for the perfect core–annular flow (see Preziosi *et al.* 1989, for instance) shows that infinitely long waves with zero wavenumbers are neutrally stable. For the eccentric cases we also calculated the eigenvalue with the maximum imaginary part as the wavenumber goes to zero. The results are shown in figure 3, when $J^* = 1000$, $m = 0.1$, $a = 0.8$ and $Re_1 = 100$. It is apparent that the imaginary part of the eigenvalue approaches zero when wavenumber of the disturbances goes to zero in both concentric and eccentric flows. A zero wavenumber corresponds to an infinite wavelength so that the neutrally disturbed flow is just another stable eccentric flow.

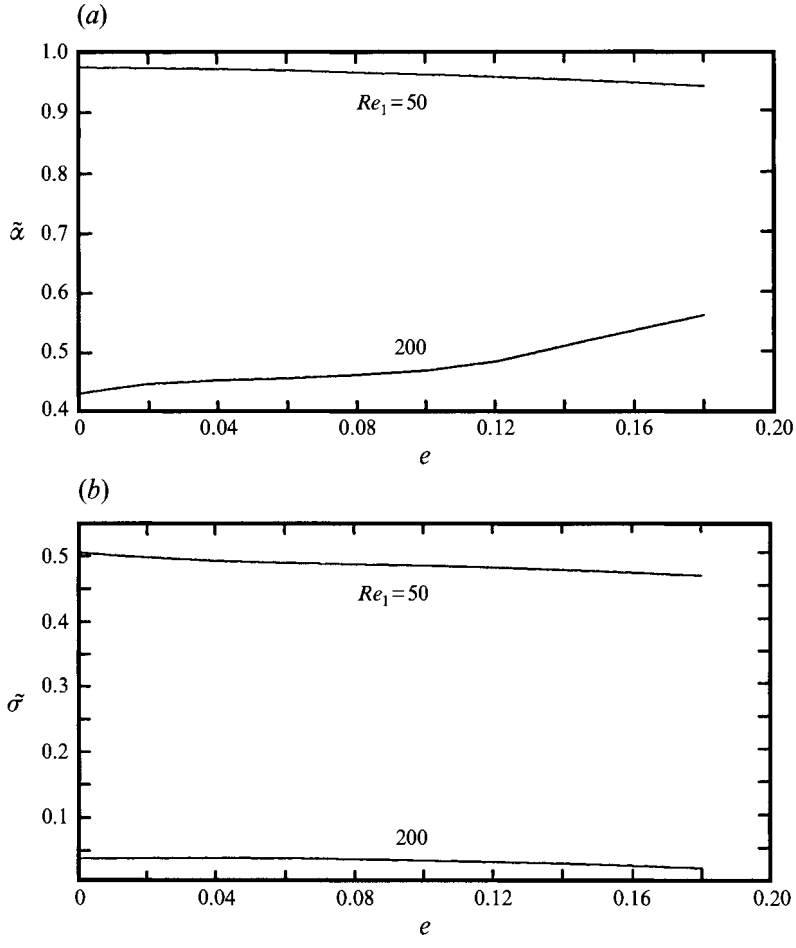

FIGURE 4. (*a*) The wavenumber $\tilde{\alpha}$ of the maximum growth rate and (*b*) the maximum growth rate $\tilde{\sigma}$, as a function of the eccentricity e, when $J^* = 5000$, $m = 0.02$, $a = 0.7$ and $Re_1 = 50$, 200.

When core–annular flow arrangements are unstable the maximum growth rate $\tilde{\sigma}$ is of great importance. $\tilde{\sigma}$ is defined as

$$\tilde{\sigma} = \tilde{\alpha} c_i(\tilde{\alpha}), \tag{42}$$

where $\tilde{\alpha}$ is the wavenumber of the most dangerous mode; the imaginary part c_i is maximum at $\tilde{\alpha}$. In practice, $\tilde{\sigma}$ is often used to predict the wavelength of the perturbed flow motion. In the case of core–annular flow, the agreement with experimental results is found surprisingly good. For the eccentric cases, we computed the maximum growth as a function of the eccentricity for some typical values of Reynolds number at which the flow is unstable. The results are shown in figure 4. Figure 4(*a*) shows $\tilde{\alpha}$ as the eccentricity increases from zero to 0.18 when $J^* = 5000$, $m = 0.02$, $a = 0.7$ and $Re_1 = 50$, 200. Figure 4(*b*) displays the corresponding growth rate. At $Re_1 = 50$, the instability is probably caused by the capillary instability, while $Re_1 = 200$ is in the region where other causes of instability dominate. These results show that eccentric cases are not qualitatively different from the concentric case. The growth rate and the wavenumber of the most dangerous mode change rather smoothly as the core is moved gradually off-centre.

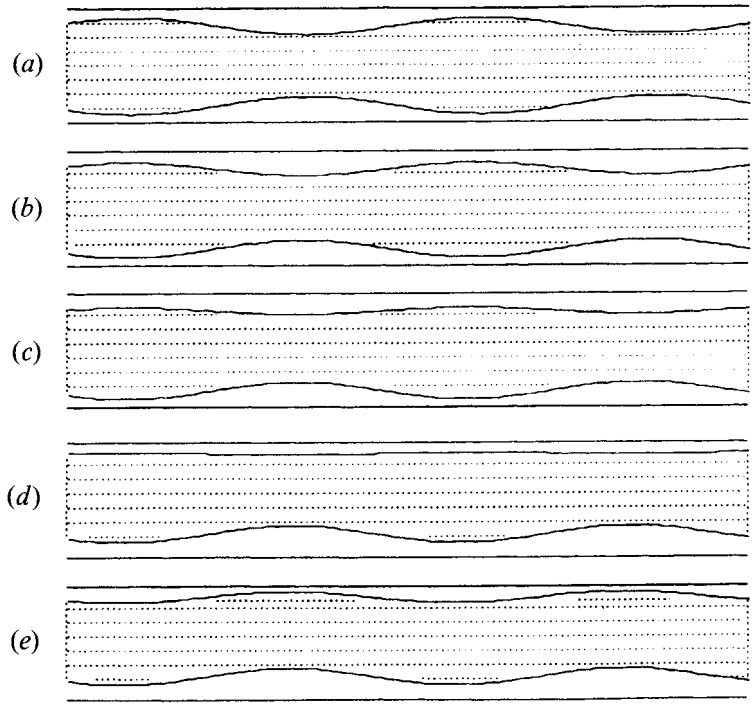

FIGURE 5. The evolution of the interfacial wave with eccentricity: (*a*) $\epsilon = 0$; (*b*) $e = 0.05$; (*c*) $e = 0.10$; (*d*) $e = 0.15$; (*e*) $e = 0.20$; $J^* = 1000$, $a = 0.7$, $m = 0.05$ and $Re_1 = 100$.

The most unstable eigenmodes for eccentric flow are, of course, not axisymmetric. In figure 5, we plot the interfacial waves associated with the most unstable eigenfunction for $J^* = 1000$, $a = 0.7$, $m = 0.05$, $Re_1 = 100$ and different values of eccentricity. Because the eigenfunctions are determined only to within an arbitrary constant, the amplitude of the eigenfunction is arbitrary in the graph. Figure 5(*a*) is for the concentric case; the interfacial wave is varicose. As the core is gradually placed off-centre, the interfacial wave evolves to the sinuous form shown in figure 5(*e*). Apart from the eccentricity, this wave form is like that associated with the asymmetric $n = 1$ mode in the concentric case, however, it is known that in the concentric case the most unstable mode is usually associated with $n = 0$, i.e. the axisymmetric mode (see Preziosi *et al.* 1989, for instance). Hence the so-called corkscrew waves observed in experiments (see Bai, Chen & Joseph 1992) are not well understood in the light of the stability analysis results for perfect core–annular flow.

We know that a real corkscrew wave is a spiral wave and does not possess mirror symmetry. But we can imagine the torques associated with nonlinear fluid motions would rotate the eccentric wave into a real corkscrew wave. The corkscrew mode in the finitely eccentric case may inherit properties of the eigenfunction belonging to the first mode of azimuthal periodicity in the concentric case. The difference between the growth rates of the varicose ($n = 0$) and sinuous modes ($n = 1$) is rather small and the ordering of the eigenvalues is sensitive to changes in the parameters. The most unstable mode in the finitely eccentric case can be regarded as a combination of modes which perturb with e the eigenfunction of the stability problem for concentric flow ($e = 0$). In this combination, the mode which reduces to the one with $n = 0$ when $e = 0$ dominates when e is small and, evidently, the mode which reduces to the one with $n = 1$ when $e = 0$ dominates for larger values of e. Thus eccentricity might just be the reason for the

appearance of the corkscrew waves in a two-phase pipeline. Finally, we note that because of the asymmetry of eccentric configuration, the corkscrew-like unstable mode is typical rather than exceptional.

7. Conclusion

We have extended the linear stability analysis of perfect core–annular two-phase pipe flow to cases when the core is off-centre. A standard linear stability analysis led us to a group of PDEs, which we solved numerically using the finite element method. To solve the resulting large asymmetric sparse eigenvalue problem we modified Saad's version of the Arnoldi projection method for applications to complex matrices. We may summarize our results as follows:

(i) Eccentricity perturbs the stability of core–annular flows continuously; there seems to be no special unstable mode due to the eccentricity of the core.

(ii) Eccentric core–annular flows can all be stable in the same open regions of parameters where concentric flow is stable.

(iii) Neutrally stable zero-wavenumber disturbances can be found for each eccentric core–annular flow. The addition of such a perfect flow and the aforementioned neutral eigenfunctions lead to a neighbouring eccentric core–annular flow.

(iv) Unstable waves superposed on eccentric flows could lead to corkscrew waves.

(v) The maximum growth rate and the associated wavenumber change continuously with eccentricity. This implies that the qualitative picture of stability and instability which has evolved from numerous studies of the concentric case carries over to the eccentric cases.

(vi) Linear stability theory does not select a stable centre for perfect core–annular flow in the density matched case. This suggests that configurations observed in practice are selected by nonlinear mechanisms. The prediction of the placement of perfect and wavy core flow with different and matched densities is not yet possible.

We find that our eigenvalue solver is a quite reliable tool. In most of our cases the dimension of the Krylov space is taken to be less than 20 and usually one pass of the Arnoldi algorithm is needed to get good convergence. Needless to say, this method is much more efficient than the routine eigenvalue solvers. However, the efficiency of this method depends directly on the bandwidths of the matrices, which is not a problem for finite difference routines. But for the finite element method, care has to be taken in numbering the nodes of the mesh in order to reduce the bandwidth.

This work was supported by grants from Department of Energy, National Science Foundation and the Minnesota Supercomputer Institute. We thank Dr Y. Saad of Department of Computer Science, University of Minnesota, for providing us with his original Arnoldi code and good advice as well, which were essential to this work.

REFERENCES

ARNEY, M. S., BAI, R., GUEVARA, E., JOSEPH, D. D. & LUI, K. 1993 Friction factor and holdup studies for lubricated pipelining I: experiments and correlations. *Intl J. Multiphase Flow* **19**, 1061–1076.

BAI, R., CHEN, K. & JOSEPH, D. D. 1992 Lubricated pipelining: stability of core–annular flow, Part 5. Experiments and comparison with theory. *J. Fluid Mech.* **240**, 97–132.

BENTWICH, M. 1964 Two-phase viscous axial flow in a pipe. *Trans. ASME* D: *J. Basic Engng* 669–672.

CHARLES, M. E., GOVIERS, G. W. & HODGSON, G. W. 1961 The horizontal pipeline flow of equal density of oil-water mixtures. *Can. J. Chem. Engng* **39**, 7–36.

CHRISTODOULOU, K. N. & SCRIVEN, L. E. 1988 Finding leading modes of a viscous free surface flow: an asymmetric generalized eigenproblem. *J. Sci. Comput.* **3**.

HU, H. & JOSEPH, D. D. 1989 Lubricated pipelining: stability of core–annular flow, Part 2. *J. Fluid Mech.* **205**, 359–396.

HUANG, A., CHRISTODOULOU, C. & JOSEPH, D. D. 1993 Friction factor and holdup studies for lubricated pipelining II: laminar and $k-\epsilon$ models of eccentric core flow. *Intl J. Multiphase flow* (to appear).

JOSEPH, D. D., NGUYEN, K. & BEAVERS, G. 1984 Non-uniqueness and stability of the configuration of flow of immiscible fluids with different viscosities. *J. Fluid Mech.* **141**, 319–345.

JOSEPH, D. D. & RENARDY, Y. 1992 *Fundamentals of Two-Fluid Dynamics, Part I.* Springer.

JOSEPH, D. D., RENARDY, M. & RENARDY, Y. 1983 Instability of the flow of immiscible liquids with different viscosities in a pipe. *Math. Center Tech. Summary Rep.* 2503.

OLIEMENS, R. V. A. & OOMS, G. 1986 Core-annular flow of oil and water through a pipeline. In *Multiphase Science and Technology*, vol. 2. Hemisphere.

PREZIOSI, L., CHEN, K. & JOSEPH, D. D. 1989 Lubricated pipelining: stability of core–annular flow. *J. Fluid Mech.* **201**, 323–356.

RUSSEL, T. W. F. & CHARLES, M. E. 1959 The effect of the less viscous liquid in the laminar flow of two immiscible liquids. *Can. J. Chem, Engng* **39**, 18–24.

SAAD, Y. 1980 Variations on Arnoldi's method for computing eigenelements of large unsymmetric matrices. *Lin. Alg. App.* **34**, 269–295.

SAAD, Y. 1989 Numerical solution of large nonsymmetric eigenvalue problems. *Computer Phys. Commun.* **53**, 71–90.

SALWEN, H. & GROSCH, C. E. 1972 The stability of Poiseuille flow in a pipe of circular cross section. *J. Fluid Mech.* **54**, 93–112.